THE ASTROPHYSICAL JOURNAL, 410:323–327, 1993 June 10

ROSAT OBSERVATIONS OF THE LMC PULSAR PSR 0540−69

JOHN P. FINLEY AND HAKKI ÖGELMAN[1]
Department of Physics, University of Wisconsin-Madison, 1150 University Avenue, Madison, WI 53706
AND
GÜNTHER HASINGER AND JOACHIM TRÜMPER
Max-Planck-Institut für Extraterrestrische Physik, Karl-Schwarzchild-Straße 1, D-8046 Garching, Germany
Received 1992 October 12; accepted 1992 December 11

ABSTRACT

The LMC pulsar PSR 0540−69, a young, rapidly rotating neutron star of dynamic age ∼1000 yr, was observed with the Position Sensitive Proportional Counter (PSPC) onboard *ROSAT* for ∼29,000 s in 1990 June, 1990 July, and 1991 February. The timing data are consistent with contemporaneous optical ephemerides suggesting that the optical and X-ray pulses are in phase. The characteristic broad sinusoidal pulse profile of PSR 0540−69 is observed at a pulsed fraction of ∼15% measured against the pulsar plus the unresolved nebula. The spectral distribution of the pulsar + nebula counts is well described by a simple power law with a photon index of $\alpha = (2.4\text{–}1.85)$ and a neutral hydrogen column density of $N_H = (3.6\text{–}4.6) \times 10^{21}$ cm^{-2} at the 90% confidence level. The implied model luminosity in the 0.1–2.4 keV band is 1.6×10^{37} ergs s^{-1} which is ∼11% of the available rotational energy loss rate and similar to the value observed in the Crab nebula + pulsar. A positive correlation between the X-ray hardness and the pulse phase intensity implies an underlying spectrum for the pulsar which is harder than the nebula. A phase-resolved spectral fit to the pulsed component supports a harder spectrum for the pulsar and gives a power-law photon index of $\alpha_{\rm pulsed} = 1.3$. The derived pulsed luminosity of 1.5×10^{36} ergs s^{-1} is ∼9% of the total X-ray luminosity.

Subject headings: Magellanic Clouds — pulsars: individual (PSR 0540−69) — X-rays: stars

1. INTRODUCTION

The 50 ms pulsar in the Large Magellanic Cloud (LMC), PSR 0540−69, was discovered in the soft X-ray band by the *Einstein* satellite in 1984 (Seward, Harnden, & Helfand 1984), and optical pulsations were subsequently observed in 1984 (Middleditch & Pennypacker 1985). The energetics, age, and morphology of PSR 0540−69 have been noted as similar to those of the Crab pulsar, but detailed comparison of pulse shape and luminosity reveal some differences (Seward et al. 1984). The optical and X-ray pulse shape of PSR 0540−69 is a broad sinusoidal feature with some smaller sharp features, while the pulse shape of the Crab pulsar is a narrow primary pulse and a secondary pulse separated by ∼0.43 in rotation phase at all wavelengths from radio through γ-ray. The fraction of the spin-down energy which emerges as pulsed X-rays in PSR 0540−69 is ∼2.5 times larger than is observed in the Crab pulsar.

Timing studies of PSR 0540−69, utilizing orbiting X-ray satellites and large optical telescopes capable of detecting the 23d magnitude pulsations, have produced measurements of $\dot{\nu}$ making it one of only three pulsars with a published braking index. Measurements of $\dot{\nu}$ have come from (*a*) *Einstein* + CTIO data (Middleditch, Pennypacker, & Burns 1987) covering the period 1979–1985; (*b*) CTIO + *Einstein* + *EXOSAT* data (Ögelman & Hasinger 1990) also covering the period from 1979 to 1985 with the *EXOSAT* data contemporaneous with the CTIO data; (*c*) *GINGA* data (Nagase et al. 1990) covering the period 1987 July–1988 October; (*d*) the Anglo-Australian Telescope (AAT) (Manchester & Peterson 1989) covering the period 1986–1988 and contemporaneous with the *GINGA* data; and (*e*) the La Silla 3.6 m telescope (Gouiffers, Finley, & Ögelman 1992, hereafter GFÖ) covering the period 1991–1992. The most recent measurement of GFÖ of $n = 2.04 \pm 0.02$ is compatible with the *GINGA* and AAT values and would seem to indicate that PSR 0540−69 is a stable rotator over periods of ≥6 yr.

The nebular component also reveals strong similarities to the Crab pulsar/nebula system. Spectral studies (Kirshner et al. 1989) indicate an expansion age of ∼760 yr based on the shift of known lines, while the abundances are consistent with those observed in the supernova remnants of other massive stars. Optical continuum emission from the nebula was discovered in 1984 by Chanan, Helfand, & Reynolds (1984) with an extent of ∼4″. The nebula contains two maxima of emission, and it is suggested that the northern, more compact one is the optical counterpart of the pulsar (Caraveo et al. 1992). Images in O III reveal an 8″ diameter shell surrounding the continuum source (Mathewson et al. 1980). The flux of the continuum emission is consistent with the extrapolation of the measured X-ray flux (Clark et al. 1982) and suggests a continuous power-law spectrum from the optical through X-ray. The observations imply a synchrotron mechanism as the source of the emission from the optical through X-ray; a conclusion which is strongly supported by the detection of a nonzero polarization from the continuum component by Chanan & Helfand (1990).

In this article we report on observations acquired during 1990 June, 1990 July, and 1991 February with the Position Sensitive Proportional Counter (PSPC) onboard *ROSAT*. The observations are described in § 2, and § 3 will contain the results of the timing analysis and the spectral analysis. Finally, a discussion of the results is found in § 4.

[1] Also at Max-Planck-Institut für Extraterrestrische Physik.

2. OBSERVATIONS

PSR 0540−69 was observed with the PSPC at the focus of the X-ray telescope onboard *ROSAT*. Detailed descriptions of the satellite, X-ray mirrors, and detectors can be found in Trümper (1983) and Pfeffermann et al. (1986). The PSPC is a gas-filled proportional counter sensitive in the energy band 0.1–2.4 keV with a resolution of $E/\Delta E \sim 2.3$ at 0.93 keV. The PSPC is mounted at the focus of an X-ray mirror assembly with a 2° field of view. The effective spatial resolution of the PSPC/X-ray mirror assembly is ~25″ at the center of the focal plane. The timing resolution, electronics-limited, is ~130 μs with an accuracy in absolute timing with respect to UTC of ~ a few milliseconds.

The observations of PSR 0540−69 which we report on here were acquired in three separate observing sessions in 1990 June, 1990 July, and 1991 February. The 1990 June data were acquired during first light of the *ROSAT* mission, while LMC X-1 was being rastered in the detector for calibration purposes. Due to the source counts being extracted from different regions of the detector, this data set was used only for timing analysis. The 1990 July data were acquired as a timing calibration target in pointed mode with instrument dithering on to prevent obscuration of sources behind support wires. The 1991 February data were from a pointed observation taken during AO1 but with the instrument dithering turned off (not by design). The observation times and effective exposure times are listed in Table 1. The three data sets were MDS (Master Data Set) and therefore free of the timing problems which are known to exist in the SASS (Standard Analysis Software System) processed data.

The source plus background counts for the 1990 July and 1991 February data were extracted from a ring of radius 2′ centered on PSR 0540−69. This extraction radius includes greater than 99% of the pulsar plus unresolved remnant counts. The background counts were extracted from an annulus of inner radius 2.′5 and outer radius 3.′3 concentric with the source. Due to its different positions within the detector during the course of the observations, the PSR 0540−69 source counts for the 1990 June data were extracted from rings of varying sizes commensurate with the point-spread function of the PSPC. The ~0.′5 spatial resolution of the PSPC did not allow a separation of the pulsar and nebula component and the extracted counts include the contributions of both. The background-subtracted counting rates in the 0.1–2.4 keV energy band, including effective area and deadtime corrections, were 0.78 ± 0.10 counts s^{-1} for the 1990 July data and 0.89 ± 0.12 counts s^{-1} for the 1991 February data. The position (J2000) of PSR 0540−69 was determined to be $\alpha = 5^h40^m9^s.9$, $\delta = -69°19'56''.3$ for the 1990 July data and $\alpha = 5^h40^m11^s.6$, $\delta = -69°20'2''.3$ for the 1991 February data. Both of these positions are in good agreement with the *Einstein*-determined X-ray position (J2000) of $\alpha = 5^h40^m11^s.03$, $\delta = -69°19'57''.5$ considering the 6″ uncertainty in the satellite attitude.

3. RESULTS

3.1. *Timing*

To ascertain the rotation frequency for each of the three data sets the photon arrival times were reduced to the Solar System Barycenter (SSBC) in the Barycentric Dynamical Time scale (TDB) utilizing the JPL DE200 ephemeris. The adopted coordinates (J2000) of PSR 0540−69 for propagation to SSBC were $\alpha = 5^h40^m11^s.03$, $\delta = -69°19'57''.5$. The Z_1^2 statistic (Buccheri et al. 1986), or, as it is often referred to in the literature, the Rayleigh Test, was calculated for a narrow range of periods bracketing the expected value as determined by extrapolation of the optical ephemeris of GFÖ Solution 1. Table 1 contains the frequencies and epochs as determined for each of the data sets. The frequency for the 1990 June data set has been previously reported by Ögelman, Hasinger, & Trümper (1992). In all three cases the determined frequency was, within errors, consistent with extrapolation of the ephemeris of GFÖ, as well as the *GINGA* ephemeris of Nagase et al. (1990). Folding of the photons at the frequency determined for each observation revealed the broad sinusoidal pulse shape which is characteristic of PSR 0540−69. The pulse profiles for each data set are presented in Figure 1. Structure at the peak of the broad pulse, which has been reported by Seward et al. (1984) in the X-ray band as well as Middleditch & Pennypacker (1985) and GFÖ in the optical band, is not apparent on either the 1990 July or 1991 February pulse but may be present on the 1990 June profile at a significance of less than 2 σ. The pulsed fractions are 14% ± 2%, 16% ± 3%, and 16% ± 3% for the 1990 June, 1990 July, and 1991 February data, respectively (we define the pulsed fraction to be mean–minimum/mean). The time of arrival (TOA) of the X-ray pulse was then determined for each of the profiles displayed in Figure 1 (the phase position for the arrival time calculation is marked by the arrow). The TOAs of GFÖ were determined for the first peak of the double-peak substructure which they observed on their optical profiles. For this reason the TOA for the 1990 June data, where substructure may be present, was chosen to correspond to the first peak to maintain consistency with GFÖ. In the case of the 1990 July and 1991 February data where no substructure is apparent, the peak of the emission was chosen for the TOA. Table 2 lists the TOAs for each observation, as well as the offset in phase from the optical ephemerides of GFÖ. The errors are for an assumed 2 ms accuracy of the *ROSAT* clock with respect to UTC, and the three solutions incorporate a ±1 pulse ambiguity in the determination of the optical ephemeris of GFÖ. Of the three TOAs listed in Table 2 the 1991 February data point is the one which is most constrained by the optical ephemeris of GFÖ. The points from 1990 June and 1990 July, while in close temporal proximity to

TABLE 1

OBSERVATIONS OF PSR 0540−69

Start (UT)	End (UT)	Exposure (s)	Epoch (JD)	Frequency[a] (Hz)
1990 Jun 16.90.....	1990 Jun 23.60	15000	2448062.1465	19.8534567 (3)
1990 Jul 18.33.....	1990 Jul 19.45	5317	2448091.7233	19.8529742 (4)
1991 Feb 20.01.....	1991 Feb 23.10	8953	2448308.9868	19.8494304 (3)

[a] Values in parentheses are the 1 σ errors in the last quoted digit.

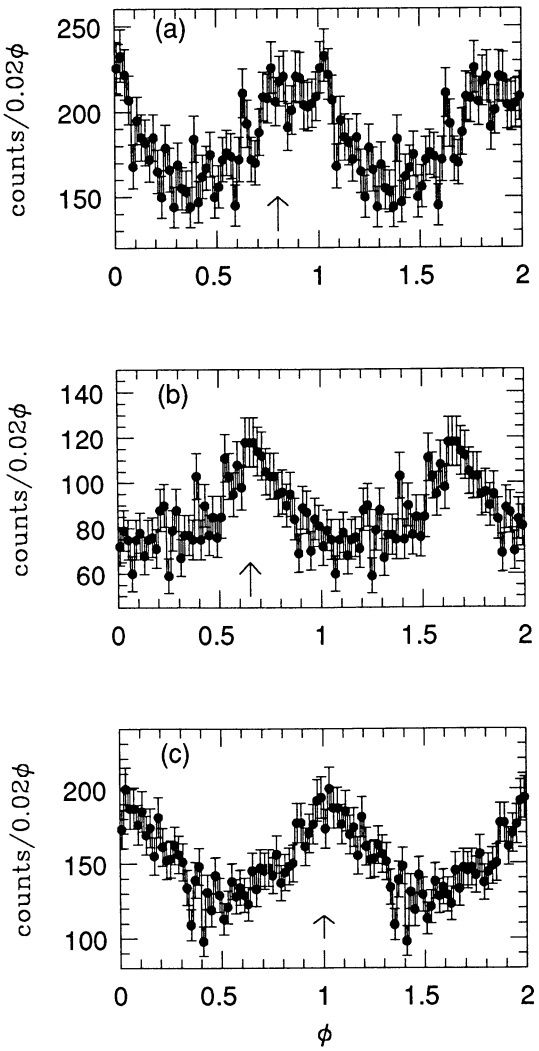

FIG. 1.—The pulse profile for PSR 0540−69 in the 0.1–2.4 keV energy band for (*a*) the 1990 June data, (*b*) the 1990 July data, and (*c*) the 1991 February data. The arrows mark the phase positions used in the determination of the TOAs listed in Table 2. Two cycles are plotted for clarity and the scales contain a suppressed zero.

each other, are not sufficiently close to the other optical data points of GFÖ to remove the pulse numbering ambiguities. It can be seen in Table 2 that the 1991 February TOA is in agreement with all three solutions of GFÖ and leads to the conclusion that the X-ray pulse and optical pulse are in phase. Additional data from the *GINGA* satellite which is contemporaneous with both the ESO optical data and the *ROSAT* data exists (J. Deeter 1992, private communication) and will allow confirmation of the phase relation of the optical and X-ray pulses.

3.2. *Spectral*

As mentioned in § 2 the spectral analysis of PSR 0540−69 excluded the 1990 June data since its constantly changing position within the detector made the correction procedure untenable. In addition, the 1991 February data was acquired with the instrument dithering turned off. This makes flux determinations unreliable as there is no way to account for obscuration by the window support wires. It does not, however, have an adverse impact on the determination of the spectral index or column density. Therefore, only the 1990 July data were utilized for flux determination while the other parameters of interest, spectral index and column density, were determined using a merged data set. The 11,813 source plus background counts from the merged data set were fitted with a power-law model ($dN/dE \propto E^{-\alpha}$) over the bandpass 0.1–2.4 keV. The χ^2 minimized at a value of 116 for the 84 degrees of freedom ($\chi^2/\mathrm{DOF} = 1.39$) for the parameters $\alpha = 2.0(+0.4; -0.15)$, and $N_H = 4.0(+0.6; -0.4) \times 10^{21}$ cm^{-2} where the errors are the 90% confidence level range. The spectrum and the best fitting model, as well as the residuals of the fit, are displayed in Figure 2. The residuals display a nonrandom behavior which are a result of known systematics which still remain in the detector response matrix (see *ROSAT* Status Report no. 10, 1992 August 1). The flux, based on the 1990 July data sample, was $F_X = (5.7 \pm 0.8) \times 10^{-11}$ ergs cm^{-2} s^{-1} which corresponds to a source luminosity, assuming a distance to the LMC of 55 kpc, of $L_X = (1.9 \pm 0.2) \times 10^{37}$ ergs s^{-1} in the 0.1–2.4 keV band.

We investigated the possibility of spectral changes as a function of the phase of the 50 ms rotation period of PSR 0540−69 in two ways. First, we defined a spectral hardness parameter as the ratio of counts in the channels 10–120 to the counts in channels 121–240. The choice of the channels was intended to yield roughly equal numbers of counts in the two bands. The pulse profiles of the 1990 July and 1991 February data were then aligned according to the TOAs which are marked in Figure 1. This hardness ratio was then evaluated as a function of the pulsar phase and the result is displayed as a correlation chart in Figure 3. The data display a positive correlation between the spectral hardness and the intensity with ~1% chance probability of arising from an uncorrelated population. The simplest interpretation of this result is that the underlying spectrum of the pulsed component is harder than the unpulsed (presumed nebular) component. Second, we attempted to construct a spectrum of the pulsed component in the following manner. Photons at the peak of the emission in pulsar phase (i.e., $\phi = 0.55$–0.75 in Fig. 1*b* and $\phi = 0.9$–0.1 in Fig. 1*c*) were chosen as "pulsed + unpulsed" photons while photons from the minimum emission region (i.e., $\phi = 0.10$–0.30 in Fig. 1*b*

TABLE 2

TIMES OF ARRIVAL FOR PSR 0540−69

TOA[a] (JD 2,440,000.0)	Δφ ESO Solution 1	Δφ ESO Solution 2	Δφ ESO Solution 3
8062.147195023 (23).....	0.28	0.03	−0.46
8091.723301524 (23).....	−0.38	0.49	−0.23
8308.986823787 (23).....	−0.03	−0.04	−0.02

[a] Values in parentheses are the 1 σ errors in the last quoted digit assuming a 2 ms accuracy of the *ROSAT* clock with respect to UTC.

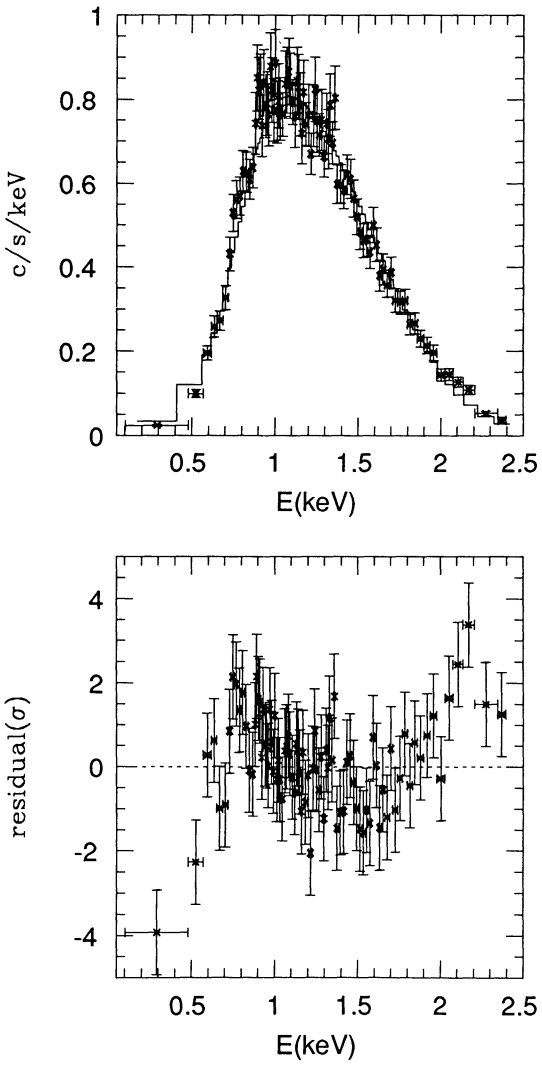

FIG. 2.—The energy spectrum of PSR 0540−69 (*upper panel*). The data points are the observed values in counts s^{-1} keV^{-1} and the histogram is the best fitting model. The lower panel are the residuals from the fit in units of σ. The nonrandom appearance is discussed in the text.

and $\phi = 0.4$–0.6 in Fig. 1*c*) were chosen as "unpulsed." This difference spectrum was then fitted to a power law with the column density fixed at the best fitting value above of 4.0×10^{21} cm^{-2}. The resulting photon index for the "pulsed" component was $\alpha_{pulsed} = 1.3 \pm 0.5$ at the 90% confidence level. The χ^2 of the fit was 1.01/DOF ($\chi^2 = 23.3$ for 23 degrees of freedom). The pulsed flux, after correcting for the fact that only a portion of the pulsed component is sampled in the above procedure, is $F_{pulsed} = (5 \pm 2) \times 10^{-12}$ ergs cm^2 s^{-1} in the 0.1–2.4 keV band corresponding to a luminosity of $L_{pulsed} = (1.8 \pm 0.6) \times 10^{36}$ ergs s^{-1}.

4. DISCUSSION

The total rotational energy loss rate of PSR 0540−69, $\dot{E} = I\Omega\dot{\Omega}$, assuming a rotational moment of inertia $I = 10^{45}$ g cm^2 is $\sim 1.5 \times 10^{38}$ ergs s^{-1}. This is a more than sufficient supply of energy to power the observed X-ray luminosity. The ratio of the energy emerging in the 0.1–2.4 keV X-ray band to the total rotational energy loss rate is $L_X/\dot{E} \sim 11\%$, similar to the value for the Crab pulsar/nebula (Harnden & Seward 1984). The 0.5

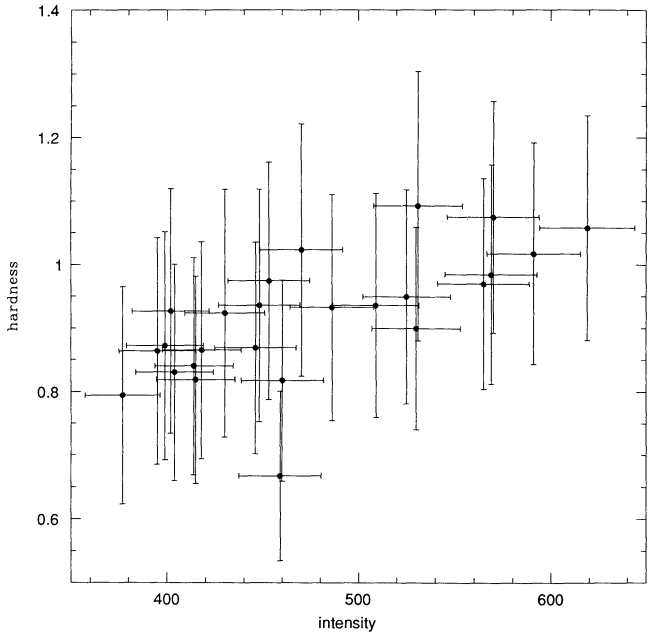

FIG. 3.—The correlation chart for the X-ray hardness (defined as the ratio of counts in channels 121–240 to the counts in channels 10–120) and the intensity. The correlations has a chance probability of ~1% of arising from an uncorrelated population.

resolution of the PSPC was too coarse to separate the pulsar and nebular components directly so we utilized the timing characteristics to estimate the pulsed luminosity. The positive correlation between the X-ray hardness and the intensity indicates that the pulsar spectrum is harder than the nebular spectrum. This is reflected by our "phase-resolved" spectral fit where we find the pulsed component described by a photon index of 1.3 as compared to the value of 2.0 for the pulsar nebula. The pulsed luminosity is ~9% of the total X-ray luminosity and about twice the fraction observed in the Crab (Toor & Seward 1977). Combining our measured pulsed flux between 0.1 and 2.4 keV of 0.9 μJy with the pulsed flux measured in the optical band (0.35–0.90 μm) by GFÖ of 7.1 μJy yields a pulsed spectrum of energy index 0.3 ± 0.1 (photon index = 1.3) which is in good agreement with the interpolation of Middleditch et al. (1987) of CTIO and *Einstein* (Seward et al. 1984) results. The fact that a single power law fits the optical through X-ray data, for both the pulsar and nebula, suggests a synchrotron emission mechanism. Indeed, measurements of the radio emission from the nebula (Mills, Turtle, & Watkinson 1978; Milne, Caswell, & Haynes 1980) display the roll-off expected due to synchrotron self-absorption of the radio photons. These data also allow us to place an upper limit to the surface temperature, T_S, of the neutron star component. If we assume that the total pulsed luminosity arises from the surface of a neutron star of radius 10 km, we derive an upper limit to the surface temperature, T_S, of $\leq 7 \times 10^6$ K. If a neutron star radius of 18 km is used, this upper limit is reduced to $T_S \leq 5.3 \times 10^6$ K. The quoted upper limits are easily accommodated by current models of neutron star cooling (see Ögelman 1991 for a review) and do not present a serious constraint.

The most striking distinction between PSR 0540−69 and the Crab is the pulse profile. In young pulsars such as the LMC pulsar and the Crab the emission is presumed to arise in the magnetosphere (Cheng, Ho, & Ruderman 1986a, b). However,

it is not clear that the magnetospheric emission models can adequately duplicate both a sharp, bipolar structure as observed in the Crab and the broad sinusoidal structure which is observed in PSR 0540−69. Another possibility for the origin of the sinusoidal profile is anisotropic heating from the neutron star interior due to nonuniform thermal conductivity of the stellar crust due to the large magnetic field ($B_S \sim 5 \times 10^{12}$ G), or a nonuniform surface emissivity due to cyclotron scattering effects (Brinkmann 1980).

In summary, the *ROSAT* observations of the LMC pulsar PSR 0540−69 have allowed us to (1) make the first attempt at determining the relative phase of the optical and X-ray pulses; (2) utilize the timing properties to ascertain the spectral character of the pulsar and nebula separately; (3) determine the spectral index of the pulsed component based solely on X-ray data.

The broad sinusoidal pulse shape of PSR 0540−69 as yet lacks a sufficient theoretical description which is still consistent with the narrow, bipolar profile observed in the Crab. While many of the characteristics of the LMC pulsar are indeed similar to the Crab the differences still remain an enigma.

This work supported by NASA grant NAGW-2643.

REFERENCES

Brinkmann, W. 1980, A&A, 82, 352
Buccheri, R., et al. 1983, A&A, 128, 245
Caraveo, P. A., Bignami, G. F., Mereghetti, S., & Mombelli, M. 1992, ApJ, 395, L103
Chanan, G. A., Helfand, D. J. 1990, ApJ, 352, 167
Chanan, G. A., Helfand, D. J., & Reynolds, S. P. 1984, ApJ, 287, L23
Cheng, K. S., Ho, C., & Ruderman, M. 1986a, ApJ, 300, 500
———. 1986b, ApJ, 300, 522
Clark, D. H., Tuohy, I. R., Long, K. S., Szymkowiak, A. E., Dopita, M. A., Mathewson, D. S., & Culhane, J. L. 1982, ApJ, 255, 440
Gouiffes, C., Finley, J., & Ögelman, H. 1992, ApJ, 294, 581 (GFÖ)
Harnden, F. R., & Seward, F. 1984, ApJ, 283, 279
Kirshner, R. P., Morse, J. A., Winkler, P. F., & Blair, W. P. 1989, ApJ, 342, 260
Manchester, R. N., & Peterson, B. A. 1989, ApJ, 342, L23
Mathewson, D. S., Dopita, M. A., Tuohy, I. R., & Ford, V. L. 1980, ApJ, 242, L73
Middleditch, J., & Pennypacker, C. 1985, Nature, 313, 659
Middleditch, J., Pennypacker, C. R., & Burns, M. S. 1987, ApJ, 315, 142
Mills, B. Y., Turtle, A. J., & Watkinson, A. 1978, MNRAS, 185, 263
Milne, J. K., Caswell, J. L., & Haynes, R. F. 1980, MNRAS, 191, 469
Nagase, F., Deeter, J., Lewis, W., Dotani, T., Makino, F., & Mitsuda, K. 1990, ApJ, 351, L13
Ögelman, H. 1991, in Neutron Stars: Theory and Observation, ed. J. Ventura & D. Pines (Dordrecht: Kluwer), 87
Ögelman, H., & Hasinger, G. 1990, ApJ, 353, L21
Ögelman, H., Hasinger, G., & Trümper, J. 1991, IAU Circ., No. 5321
Pfeffermann, E., et al. 1986, SPIE, 733, 519
Seward, F. D., Harnden, F. R., Jr., & Helfand, D. J. 1984, ApJ, 287, L19
Toor, A., & Seward, F. D. 1977, ApJ, 216, 560
Trümper, J. 1983, Adv. Space Res., 2, 241